ORIGINAL ARTICLE

Strontium substitution of gelatin modified calcium hydrogen phosphates as porous hard tissue substitutes

Benjamin Kruppke[1] [ORCID] | Christiane Heinemann[1] | Annett Gebert[2] | Marcus Rohnke[3] | Manuel Weiß[3] | Anja Henß[3] | Hans-Peter Wiesmann[1] | Thomas Hanke[1]

[1]Institute of Materials Science, Max Bergmann Center of Biomaterials, Technische Universität Dresden, Dresden, Germany

[2]Institute for Complex Materials, Leibniz-Institute for Solid State and Materials Research Dresden (IFW Dresden), Dresden, Germany

[3]Institute of Physical Chemistry, Justus-Liebig-Universität Gießen, Gießen, Germany

Correspondence
Benjamin Kruppke, Max-Bergmann-Zentrum für Biomaterialien, Budapester Straße 27, 01069 Dresden, Germany.
Email: benjamin.kruppke@tu-dresden.de

Funding information
Research Foundation; Deutsche Forschungsgemeinschaft

Abstract

Aiming at the generation of a high strontium-containing degradable bone substitute, the exchange of calcium with strontium in gelatin-modified brushite was investigated. The ion substitution showed two mineral groups, the high-calcium containing minerals with a maximum measured molar Ca/Sr ratio of 80%/20% (mass ratio 63%/37%) and the high-strontium containing ones with a maximum measured molar Ca/Sr ratio of 21%/79% (mass ratio 10%/90%). In contrast to the high-strontium mineral phases, a high mass loss was observed for the calcium-based minerals during incubation in cell culture medium (alpha-MEM), but also an increase in strength owing to dissolution and re-precipitation. This resulted for the former in a decrease of cation concentration (Ca + Sr) in the medium, while the pH value decreased and the phosphate ion concentration rose significantly. The latter group of materials, the high-strontium containing ones, showed only a moderate change in mass and a decrease in strength, but the Ca + Sr concentration remained permanently above the initial calcium concentration in the medium. This might be advantageous for a future planned application by supporting bone regeneration on the cellular level.

KEYWORDS
biomimetic material, calcium phosphate, degradation, strontium phosphate, ion release

1 | INTRODUCTION

Investigations on new biomaterials to restore the biochemical functions and mechanical properties of human hard tissue, such as bone, are often focused on so-called bioinspired or biomimetic materials.[1] The combination of organic and inorganic components allow the transfer of structures from a variety of organic templates to the inorganic component, which leads to otherwise unattainable inorganic morphologies and structures.[2-4] Thus, the property of degradability in terms of physicochemical dissolution was put in focus, in order to provide biomaterials that can be incorporated into the bone remodeling process. Calcium phosphates and their composites containing organic templates are one group of these materials, which have been developed as increasingly better biomimetics of bone. An example for these are the basic research on apatite crystal formation under influence of gelatin reported by Kollmann et al.,[5] which provides a basis for the material precipitation process used.

The mineral phases monetite and brushite, also known as anhydrous and dihydrous calcium hydrogen phosphate, are commonly described and investigated in terms of calcium phosphate cements.[6,7] These are used for defect filling of large hard tissue defects. Compared with their relatives, the hydroxyapatite-hardening calcium

phosphate cements, the monetite and brushite cements are generally characterized by a higher resorbability.[8-10] Due to metastability of brushite in physiological conditions, it is not only resorbed during the natural remodeling process but also degraded by physicochemical dissolution.[11] Furthermore, it is important to point out that brushite scaffolds degrade slower than monetite scaffolds owing to the initial conversion of brushite into apatite.[12]

The minerals can be synthesized in vitro by simple precipitation, as has been done here with a modification of this process by adding gelatin. The resulting material, described earlier and named PPGC (phosphate pre-structured gelatin mineralized with calcium), showed promising potential as bone substitute material with respect to osteoblastic differentiation and especially osteoclastic resorbability.[13] The material inherent mechanisms of action are in the focus of mineral synthesis, in such a way that a targeted adjustment of material degradation enables the release of ions to manipulate cells during bone remodeling. To this end, therapeutic metal ions (such as calcium, strontium, copper, zinc) have moved into the focus of bone substitute material modification.[14] The use of such ions represents a potential alternative to more expensive, highly sensitive, and potentially dangerous biomolecules, such as growth factors.

To support bone remodeling and manipulate the ratio of osteoblastic and osteoclastic cells, it was the aim to introduce strontium in the precipitation process of the so called PPGC-minerals. Strontium has previously been investigated as an active agent ingredient in case of strontium ranelate as well as in biomaterials such as strontium phosphate and carbonate and has demonstrated its capability of stimulating bone formation.[15-19]

A therapeutic effect of strontium in bone regeneration has been investigated by Marie et al., revealing beneficial effects on bone cells and bone formation in vivo.[17] Positive effects on bone mass after strontium and strontium ranelate administration in case of postmenopausal osteoporosis were observed in several studies.[17,20,21] The review by Neves et al.[22] provides a good overview of current in vivo studies on the effects of strontium released from biomaterials. Here the advantages of the strontium effect with those of a local release become clearly visible. However, there is still no biomaterial that can absorb such a large concentration range of strontium as the scaffolds presented in the present article, and yet can be processed from a pure mineral powder to a specimen or scaffold for in vitro and in vivo testing.

An influence of different extracellular strontium ion concentrations in cell culture medium on osteogenic behavior of bone marrow stromal cells, periodontal ligament cells, (pre-)osteoblasts and more has been presented in previous studies in the literature.[23-27]

The bone anabolic effect of Sr at the cellular level was shown to be dependent on the strontium ion concentrations. Bizelli-Silveira et al., showed recently enhanced proliferation and osteogenic differentiation in vitro of periodontal ligament cells as well as bone marrow stromal cells of mesenchymal and ectomesenchymal origins when the medium was supplemented with 360 mg/L of Sr (4.1 mM, $SrCl_2·6H_2O$), which is 30 times of human serum concentration reached after common Sr systemic supplementation used by osteoporotic women (13 mg/L).[25,26] Verberckmoes et al., showed in an in vitro primary rat osteoblast culture, that strontium concentrations of 2 to 5 μg/ml ($2.3–5.7 × 10^{-3}$ mM, $SrCl_2·6H_2O$) do not change mineral formation and stimulate osteoblastic differentiation, while higher concentrations (0.2–1.1 mM) did not influence osteoblast differentiation but disturbed mineral formation.[23]

Furthermore, Bonnelye et al. revealed a significant increase in mRNA expression of the osteoblastic markers supplementing a mouse calvaria cell culture with 0.1–1.0 mM Sr (Sr ranelate).[24] Additionally, they were able to show the strontium ranelate induced dose-dependent decrease in osteoclast differentiation, starting at 0.1 mM and total inhibition of osteoclast formation at 24 mM Sr.[24]

Own investigations on osteoblast proliferation and differentiation in solely strontium containing medium lacking of calcium revealed optimal concentrations of 0.9–1.8 mM strontium.[28] Therefore, there is a need for the examination of bone substitute materials with a high strontium content. In the present article we show how strontium ions can be easily integrated into an established calcium phosphate material concept, as represented by gelatin modified calcium hydrogen phosphates, and what effect they have on biomaterial degradation and mechanical stability during incubation in the cell culture medium.

2 | MATERIALS AND METHODS

2.1 | Mineral precipitation and specimen preparation

The precipitation of gelatin modified calcium/strontium phosphates is based on a process we have described previously.[13] In the present study, the focus was put on two main influences, firstly that of strontium on the mineral precipitation and secondly the strontium effect on material degradation and mechanical stability.

In brief, the mineral precipitation was performed as follows (Figure 1). First, porcine gelatin (300 bloom, 20 meshes, Gelita) was suspended in deionized water (0.9%) und liquefied by heating in a water bath (50°C). According to the manufacturer, the gelatin has less than 2% residues after loss on ignition (550°C) and contains in total less than 100 mg/kg of heavy metals. The water content is 9.0–13.0%. A Na_2HPO_4 (Roth) solution was added to reach a final concentration of 0.106 M and the pH was adjusted to 7.0 ± 0.1 by 3 M HCl. For phosphate pre-structuring of gelatin the solution (850 ml) was stored at least 8 hr. For mineral formation, 1 M cationic mineralization solutions (250 ml) were prepared of $CaCl_2·2H_2O$ (Roth), $SrCl_2·6H_2O$ (Roth). The ratio of calcium to strontium ion concentration (x:y) was set to 10:0, 9:1, 5:5, 3:7, 1:9, and 0:10, respectively. The mineralization solutions were added with 2.5 ml/min to the phosphate gelatin solution. After complete addition of mineralization solutions, the suspension was stirred for ripening for 3 hr. During this time, the pH drops from 7.0 to 4.5–4.0. The resulting gelatin modified minerals are named C 10:0 (pure calcium containing mineral), S 0:10 (pure strontium containing mineral) and C + S x:y for the mixed mineralization solutions, with the above mentioned Ca/Sr ratios. After
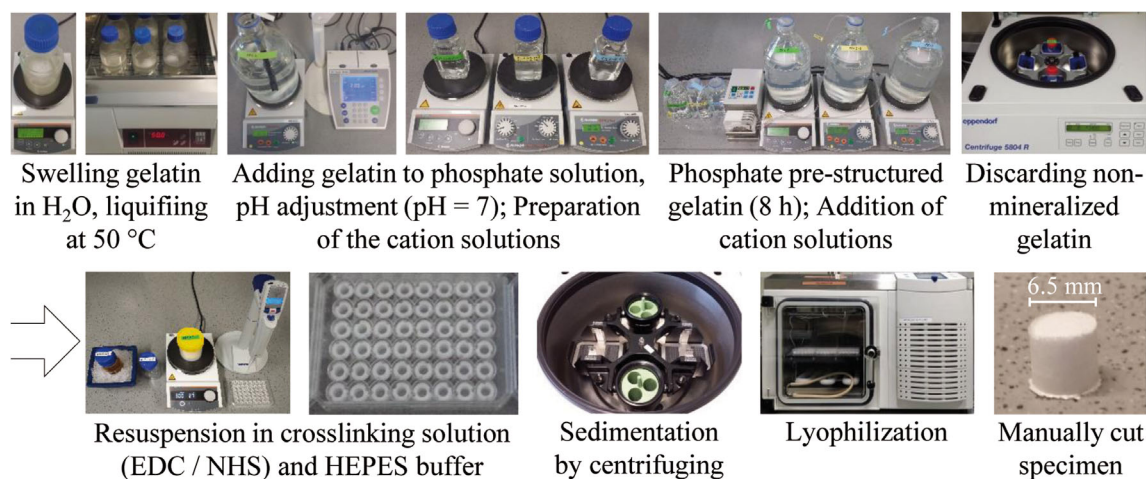
FIGURE 1 Photographs of gelatin modified mineral precipitation and specimen preparation procedure

ripening, the mineral was separated from the supernatant by centrifugation (3,000 rcf, 5 min) and discharging of all nonturbid supernatant.

Preparation of porous specimen was performed by sedimentation (Figure 1, lower row). Therefore, 2 g of the mineral pellet obtained after ripening and centrifugation was resuspended in 1 ml 0.5 M HEPES puffer (pH = 8.0, Roth) and 0.5 ml 300 mM 1-Ethyl-3-(3-dimethylaminopropyl) carbodiimide (EDC, Sigma-Aldrich) and 150 mM N-Hydroxysuccinimide (NHS, Sigma-Aldrich). Afterwards, 450 μl of the suspension was transferred to a 48 well plate with hollow cylindrical PTFE inserts, with an inner diameter of 6.5 mm. The well plates were centrifuged (1900 rcf, 10 min) and kept for crosslinking for at least 8 hr at 8°C. The specimen were lyophilized and afterwards pushed out of the well inserts to be cut manually to a height of about 3.5 mm with a scalpel. The specimen initial dry masses were measured with an analytical balance (BP211D, Sartorius). The open porosity of the final specimens was measured by ethanol infiltration under vacuum. The mass of the ethanol absorbed was measured with a moisture analyzer (MA 60.3Y, Radwag) and converted to volume. The porosity was calculated in relation to the volume of the specimen volume.

Finally, half of the specimen were sterilized by gamma irradiation (25 kGy, Synergy Health) to separately investigate the influence of gamma irradiation on degradation and mechanical stability.

2.2 | Mineral characterization: Scanning electron microscopy, Fourier transform infrared spectroscopy, X-ray diffraction, and optical emission spectrometry with inductively coupled plasma

The morphology of the synthesized minerals as well as of the final specimen was analyzed by scanning electron microscopy (Philips XL30 FEG) with 3 kV acceleration voltage. Mineral powder was spread on a sample holder with a carbon tab and coated with carbon in a Balzers SCD 050 coater.

Additionally, phase analyses and crystal structure of the minerals were performed using Fourier transform infrared spectroscopy (FT-IR)

and X-ray diffraction (XRD). Therefore, the specimens were placed on a universal attenuated total reflectance (UATR) unit and spectroscopy was performed with a step width of 1 cm^{-1} and 4 single scans in the finger print range of 500–2000 cm^{-1} with a Spectrum Two FT-IR (Perkin Elmer).

X-ray diffraction measurements of pelletized samples were conducted using a PANalytical Emypyrean powder diffractometer in Bragg–Brentano $\theta-\theta$ geometry with a PIXcel^{3D} area detector. The Cu Kα X-ray source ($\lambda_1 = 1.5405980$ Å, $\lambda_2 = 1.5444260$ Å, $I(\lambda_2)/I(\lambda_1) = 0.5$) was operated at 40 mA emission current and 40 kV acceleration voltage. Data were recorded in the 2θ range between 10° and 70° with a step size of 0.013° and 300 s counting time per step. Only the C 10:0 and C + S 9:1 samples exhibited adequate crystallinity for Rietveld refinement (see Supplement A - Structural characterization; Figure S1: Laboratory X-ray diffraction data, Table 1: Structural parameters from the refinement of X-ray diffraction data of a sample with nominal composition CaHPO4 [C 10:0] and Table 2: Structural parameters from the refinement of X-ray diffraction data of a sample with nominal composition Ca0.9Sr0.1HPO4 [C + S 9:1]). The measurements of the other samples were only used for identification of the crystalline phase.

Optical emission spectrometry with inductively coupled plasma (ICP-OES) was used for quantitative element analysis of the precipitated minerals. The test specimens were first completely dissolved in nitric acid and then at least 12 sample solutions were tested to determine the emission spectra with an iCAP 6,500 Duo View (Thermo Fisher Scientific). Sample aerosol was sprayed in a hot argon plasma and emission of characteristic electromagnetic radiation after excitation of ions was used to identify the elements contained in the sample and to determine their mass fraction in the sample.

2.3 | Degradation

For degradation investigations six cylindrical specimen (d = 6.5 mm, h = 3.5 mm) were stored in cell culture medium in a static regime.

TABLE 1 Structural parameters from the refinement of X-ray diffraction data of a sample with nominal composition CaHPO$_4$ (C 10:0)

Atom	x/a	y/b	z/c	B_{iso}/Å^2	N
Ca1	0.78(4)	0.3266(4)	0.49(4)	1.3	1.0
P1	0.25(4)	0.3151(5)	−0.03(4)	1.4	1.0
O1	0.32(4)	0.39218(14)	0.17(4)	3.3	1.0
O2	0.66(4)	0.3032(11)	0.13(4)	1.7	1.0
O3	0.27(4)	0.3690(12)	−0.21(4)	0.9	1.0
O4	0.04(4)	0.242(2)	−0.07(4)	2.1	1.0
O5	0.76(4)	0.4199(14)	0.72(4)	3.3	1.0
O6	0.90(4)	0.4390(11)	0.34(4)	0.2	1.0
H1	0.1568	0.3293	0.2897	4.0	1.0
H2	0.6427	0.4898	0.7482	4.0	1.0
H3	0.4647	0.4121	0.7452	4.0	1.0
H4	0.7785	0.5094	0.2794	4.0	1.0
H5	0.756	0.4334	0.1167	4.0	1.0

Note: Obtained lattice parameters: a = 5.8248(4) Å, b = 15.1966(6) Å, c = 6.2573(4) Å, β = 116.411(4)°. Refined mass fractions: 93.9(5) % brushite, 6.1(5) % hydroxyapatite; goodness of fit S = 2.82, R_p = 7.75%, R_{wp} = 10.51%, R_{exp} = 3.72%.

TABLE 2 Structural parameters from the refinement of X-ray diffraction data of a sample with nominal composition Ca$_{0.9}$Sr$_{0.1}$HPO$_4$ (C + S 9:1)

Atom	x/a	y/b	z/c	B_{iso}/Å^2	N
Ca1	0.62(2)	0.3299(4)	−0.11(3)	0.7(4)	1.00(3)
Sr1	0.62(2)	0.3299(4)	−0.11(3)	0.7(4)	0.00(3)
P1	0.13(2)	0.3184(5)	0.07(3)	0.7(4)	1.0
O1	0.05(2)	0.3831(14)	0.04(3)	1.6(8)	1.0
O2	0.38(2)	0.2870(10)	−0.31(3)	0.2	1.0
O3	0.04(2)	0.3789(13)	−0.21(3)	0.4	1.0
O4	−0.12(2)	0.2333(13)	0.58(3)	1.0	1.0
O5	0.45(2)	0.4304(13)	0.16(3)	2.5(6)	1.0
O6	0.64(2)	0.4415(12)	−0.11(3)	1.0(7)	1.0
H1	0.1568	0.3293	0.2897	4.0	1.0
H2	0.6427	0.4898	0.7482	4.0	1.0
H3	0.4647	0.4121	0.7452	4.0	1.0
H4	0.7785	0.5094	0.2794	4.0	1.0
H5	0.756	0.4334	0.1167	4.0	1.0

Note: Obtained lattice parameters: a = 5.8304(2) Å, b = 15.2186(6) Å, c = 6.2705(3) Å, β = 116.369(3)°. Refined mass fractions: 100% brushite; goodness of fit S = 1.75, R_p = 4.37%, R_{wp} = 5.71%, R_{exp} = 3.26%.

Therefore, the specimen were incubated in 8 ml liquid each and kept there for 28 days. The medium, α-minimal essential medium (α-MEM, Biochrom), was supplemented with 10% fetal calf serum (FCS, Biochrom), 100 U/ml penicillin, 100 μg/ml streptomycin (1% penicillin/streptomycin, Biochrom), and 2 mM L-glutamine. The specimen were stored in an incubator (Heracell, Heraeus) at 37°C and 5% CO$_2$. The degradation was measured by weighing the specimen (BP211D, Sartorius) before and after incubation and drying to constant mass (about 4 days at 37°C, 15% humidity in an incubator). For analysis of ion concentrations 1 ml liquid samples were taken of the medium without replacement after 1, 7, 14, 21, and 28 days. At each time point calcium and strontium ion concentration was measured as a combined cation concentration using a colorimetric Fluitest® CA CPC test kit (Analyticon) and an Infinite 200 Pro microplate reader (Tecan). Detailed information on the method of combined measurement of cations is given in the Supplement B - Ca/Sr assay (Figure S2: Absorption of Fluitest® CA CPC for dilution series of Calcium and Strontium solutions). For phosphate ion concentration the same was done using the colorimetric Fluitest® PHOS test kit (Analyticon). The pH was determined using a single rod glass electrode (InLab Micro, Mettler Toledo) and the pH meter Seven Multi (Mettler Toledo) at room temperature and ambient atmosphere.

2.4 | Mechanical strength

For determination of the tensile strength the indirect method of the Brazilian test was used to analyze six cylindrical specimens each with 6.5 mm diameter and about 3.5 mm height. The material was subjected to two opposing normal strip loads at the cylinder's pile skin surface. The tests were performed with an Instron 5566 (Instron) universal testing machine. The load was applied with 0.5 mm/min and the maximum force F leading to fracture was used to calculate the indirect tensile strength β_{SZ} based on the following equation with cylinder diameter d and cylinder height h: $\beta_{SZ} = 2F/(\pi \cdot d \cdot h)$.

2.5 | Statistics

All measurements were performed in triplicate and are expressed as means ± *SD*. Results were tested for significant differences by two-way analysis of variance (ANOVA) with Bonferroni post hoc test, where applicable. In this article a significance level of 5% is marked with one star (*). In order not to provoke the first type error, only data for which an effect is expected are tested.

3 | RESULTS

3.1 | Variation of particle morphology and composition as function of Ca/Sr ratio

The variation of the Ca/Sr ratio in the mineralization solutions led to a change in the characteristic particle morphology visible for both pure mineral phases C 10:0 and S 0:10 (Figure 2). The platelet-shaped crystals of C 10:0 have ~50–100 μm length and width, respectively, and became smaller owing to an increasing amount of strontium. Already at a ratio of 10% strontium chloride and 90% calcium chloride in the
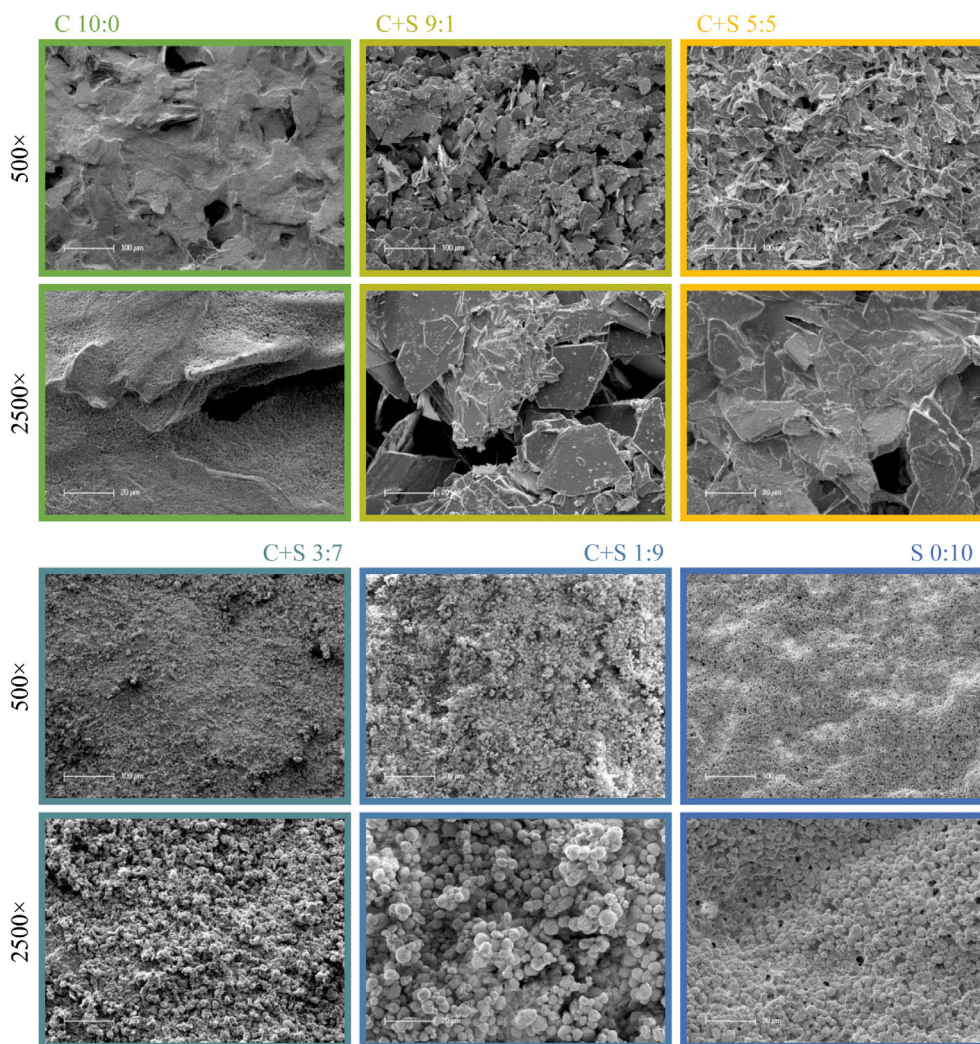
FIGURE 2 SEM images of the particle morphology of the dried minerals after precipitation at magnifications of ×500 and ×2,500

mineralization solution (C + S 9:1), the particles have dimensions of less than 50 µm. Starting from the pure strontium phosphate (S 0:10) the morphology is altered slightly by the addition of calcium ions. The S 0:10 particles have a regular spherical shape with diameters of ~5–10 µm.

The specimen made from the mineral had initial dry masses of about 53 mg (C 10:0) to 106 mg (S 0:10), respectively. The specimen masses (Figure 3) showed a dichotomy of the mineral phases (C 10:0, C + S 9:1, C + S 5:5 and C + S 3:7, C + S 1:9, S 0:10), each showing a correlation of increasing mass with increasing proportion of strontium, which has a molecular mass more than twice as high as calcium. This affects the mass of the specimens of equal volume. The porosity (mean ± SD) of the specimen showed no statistically significant differences ranging from 75.9 ± 1.5% (C 10:0) to 70.8 ± 4.0% (S 0:10).
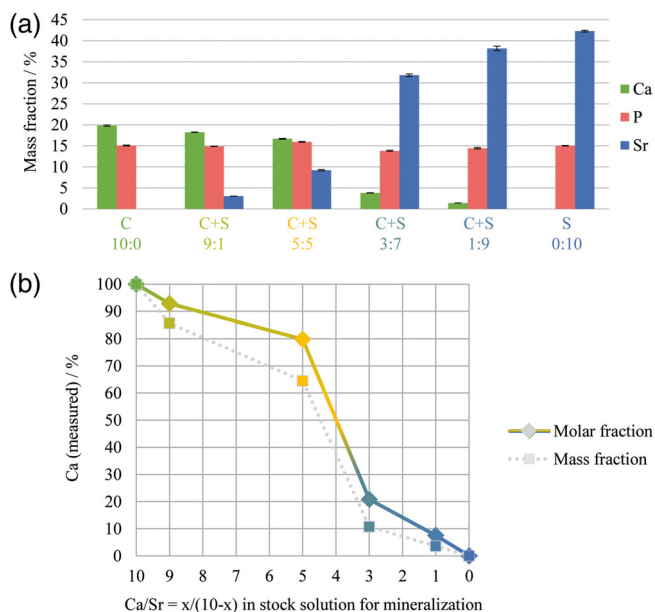
Using ICP-OES, the test specimens were examined for their elemental masses of calcium, strontium, and phosphorus. The calcium content in the specimens C 10:0, C + S 9:1, and C + S 5:5 was between 15 and 20 wt% and decreased with increasing amount of strontium in the mineralization solution (Figure 4a). In comparison, the strontium mass of C + S 3:7, C + S 1:9 and S 0:10 was above 30 wt%
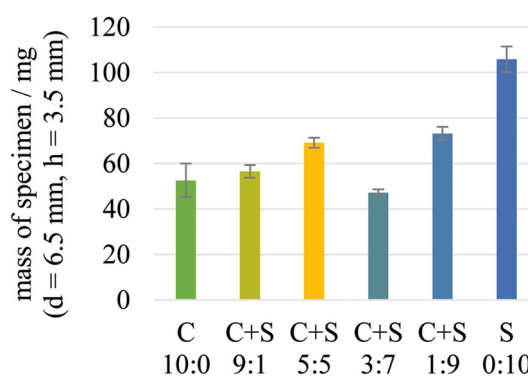

FIGURE 3 Mass of specimen prepared from different minerals. Error bars indicate SD

and increased according to the amount of substitution. The phosphorus mass remained constant at ~15 wt% for all specimens.

Furthermore, a correlation between the mineral composition (molar and mass ratio of Ca to Sr) and the calcium or strontium ion concentrations in the mineralization solution can be observed. In

FIGURE 6 Mineral analysis of specimens by XRD with brushite (RRUFFID = R070554), hydroxyapatite (RRUFFID = R060180), monetite,[29] and SrHPO4 (JCPDS 12–0368 according to[30-32]) as reference (b)
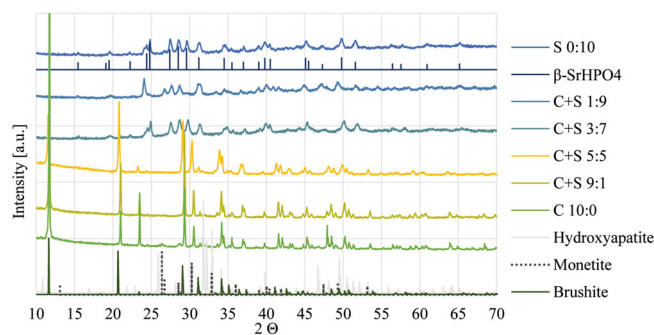

FIGURE 4 Element proportions of Ca, P, Sr determined by ICP-OES as a function of material composition (a) and molar as well as mass fractions of the elements Ca and Sr determined from ICP-OES measurements (b). Error bars indicate standard deviation
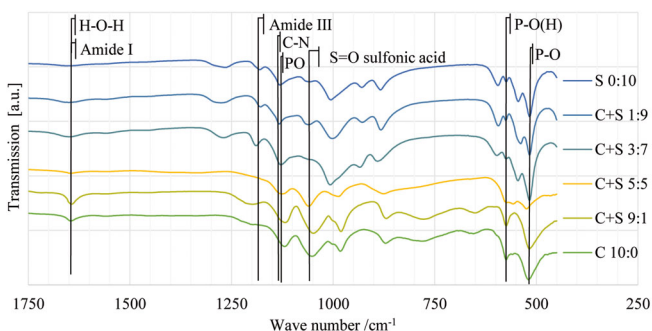
FIGURE 5 Mineral analysis of specimens by UATR FT-IR

Figure 4b, the calcium quantities measured by ICP-OES are shown as a function of the Ca/Sr ratio used for mineralization. From this it can be concluded that there is no linear substitution of calcium ions by strontium ions in the mineral. Starting from C 10:0 a substitution with up to 35 wt% strontium (molar fraction 20%) is possible in case of C + S 5:5. Starting from the other end of the material composition—S 0:10—a substitution of strontium by calcium of about 10% by mass (molar fraction 21%) can be measured in the case of C + S 3:7.

UATR FT-IR spectrometry of the specimen revealed high similarity on the one hand of C 10:0, C + S 9:1, and C + S 5:5 with each other as well as on the other hand of C + S 3:7, C + S 1:9, and S 0:10 (Figure 5). Despite the fact that clear differences can be seen in the fingerprint range between these two groups, for example, at 1270, 930, and 590 cm^{-1} in all spectra the phosphate bands are evident at 1125, 575, and 515 cm^{-1}. The gelatin related amide bands are present

at 1,645 cm^{-1} (amide I) and 1,190 cm^{-1} (amide III). The S=O stretching absorption at 1,070–1,030 cm^{-1} indicates sulfonic acid groups of HEPES retained from the preparation in the specimens.
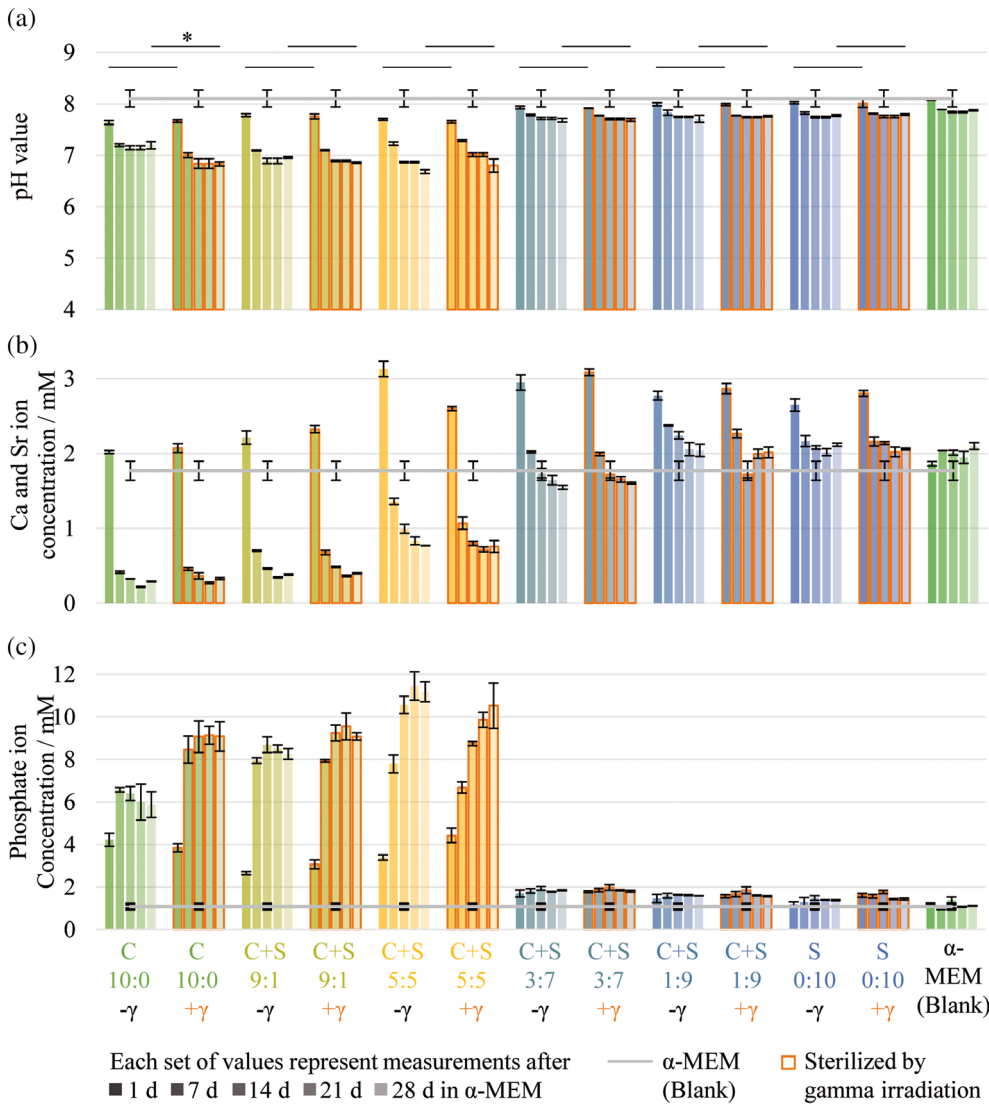
In accordance with ICP-OES, FT-IR, and SEM, the samples showed in structural analysis by XRD a high similarity between C 10:0, C + S 9:1, and C + S 5:5 on the one hand and C + S 3:7, C + S 1:9, and S 0:10 on the other (Figure 6).

The calcium-rich minerals (C 10:0, C + S 9:1, C + S 5:5) showed main peaks of monoclinic brushite space group $I1a1$ (International tables #9).[33] TOPAS-Academic V6[34] was used for structural analysis. For S 0:10 (Figure 6) an agreement with γ-SrHPO4 in der Raumgruppe Pbca (ICSD 91129) was found. Furthermore, the assignment of SrHPO4 (ICDD # 00-012-0368) was made according to the publications of Wang et al., Zhuang et al. and Roming et al..[30-32]

3.2 | Influence of mineral composition and gamma sterilization on ion release, changes in mass and mechanical strength during storage in medium

Sterilization of biomaterials is a necessary step for their application in the presence of cells. Its disadvantage is that gamma rays can cross-link polymers and also cleave them. As can be seen from both Figure 7 and Figure 8, all sample variants showed no significant changes in degradation after gamma sterilization.

According to Figure 7a the pH values after sterilization for C 10:0, C + S 9:1, C + S 5:5, C + S 3:7, C + S 1:9 and S 0:10 do not differ significantly (tested at day 1 and 28 for each material group) from those without gamma irradiation with one exception (C 10:0 at day 28). The pH values indicate two material groups. Samples with higher calcium contents (C 10:0, C + S 9:1, and C + S 5:5) caused a significant pH reduction from day 1 to day 28 compared to the reference medium without sample. In these specimens, the pH reduction was slightly increased after sterilization. Test specimens with higher strontium contents (C + S 3:7, C + S 1:9, and S 0:10) reduced the pH value only slightly. The slight decrease in pH values were in the range of the reference medium (Figure 7a; right bar group).

(a)

(b)

(c)

Each set of values represent measurements after — α-MEM (Blank) □ Sterilized by
■ 1 d ■ 7 d ■ 14 d ■ 21 d ■ 28 d in α-MEM gamma irradiation

Release of cations in the medium prove that gamma sterilization has no influence on the ion release as well. After an initial ion release at day 1 the cation concentration was reduced further on by samples with higher calcium contents (C 10:0, C + S 9:1, and C + S 5:5) as a function of their Ca/Sr ratio in the test specimen. The maximum initial ion release was present for the mixed phases C + S 5:5 and C + S 3:7. For C + S 1:9 and S 0:10 the cation concentration was above the initial concentration of the blank for the whole time of incubation.

The colorimetrically determined release of phosphate ions also showed two distinct groups. The test specimens with higher calcium contents (C 10:0, C + S 9:1, and C + S 5:5) caused a significant increase in the phosphate concentration up to 6 mM (C 10:0) and 11 mM (C + S 5:5), respectively, in comparison to 1.1 mM of the blank medium. The phosphate concentration was increased comparatively little to values between 1 and 2 mM by the test specimens with higher strontium contents (C + S 3:7, C + S 1:9, and S 0:10).

In addition to the ion release, the change of the specimens' masses were determined as a characteristic of their degradability. The measurements represent the dissolution of the specimens, which may

be superimposed by the precipitation of calcium phosphate phases from the medium on the specimens. The latter leads to an increase in mass and thus to a measured degradation which is lower than the real one.

The changes in mass of the specimens showed that gamma sterilization has no significant influence on degradation (Figure 8a). All material variants exhibited mass decrease during storage in static cell culture medium. The mass decrease of the more strontium-containing specimens (C + S 3:7, C + S 1:9, and S 0:10) always took place during the first day. Afterwards, the test specimen masses remained almost constant over the storage period. With increasing calcium substitution of S 0:10, the initial decrease in mass intensified. At the other end of the material spectrum (C 10:0), the mass decreased after 14 days to ~72% referenced to the initial mass and remained at this value until day 28. C + S 5:5 showed a very continuous decrease in mass over time to 78%.

Of course, it is to be assumed that in the case of degradation the strength of test specimens decreases. In the case of re-precipitation from electrolyte solutions, the strength may also increase again. For

FIGURE 8 Each set of values from left to right describes the change over time with measurements of the initial dry state (0 day) and after 1, 14, and 28 days in α-MEM. (a) Relative mass and (b) indirect tensile strength of dried specimens without (−γ) and with (+γ) gamma sterilization. Degradation by static ageing in α-MEM over 28 days. Error bars indicate standard deviation. Influence of gamma irradiation was analyzed statistically for all material subgroups in dry state and after 28 days
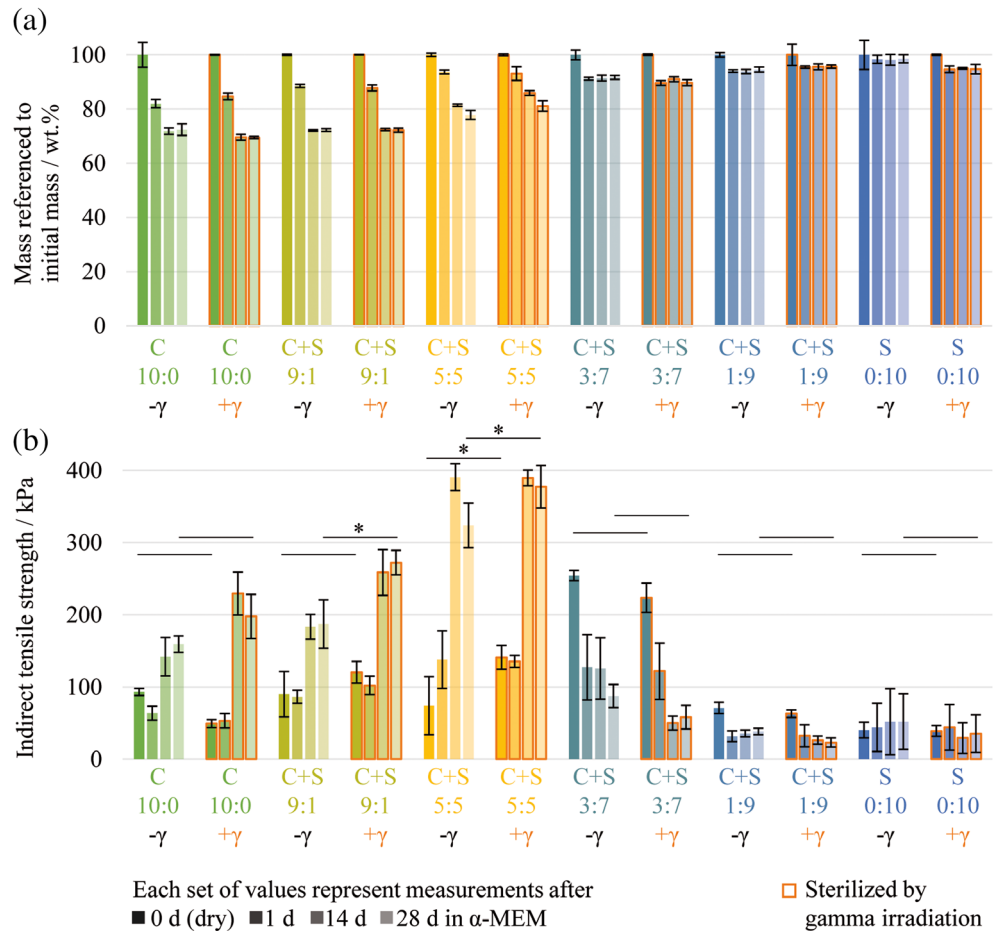
this reason, investigations were carried out regarding the development of the indirect tensile strength as a function of the degradation time. According to Figure 8b, it can be seen that gamma sterilization causes only in minor cases (3 of 12 tested subgroups) statistically significant changes in mechanical strength. Figure 8b shows that the strength alterations of specimens rich in calcium and strontium differ significantly. The test specimen strength of C 10:0, C + S 9:1, and C + S 5:5 increases up to four times the initial value during storage. The increase in strength in the wet state was only measurable from day 14 for C 10:0, C + S 9:1, and C + S 5:5. The maximum strength attained was almost 400 kPa for C + S 5:5 after 14 days of incubation. The highest initial strength was achieved in case of C + S 3:7 with 254 kPa (nonsterile) and 223 kPa (sterile), while it dropped to 87 and 58 kPa during incubation, respectively. The test specimen strength remained constant at a very low initial level in the case of S 0:10.

4 | DISCUSSION

4.1 | Morphology and composition of gelatin-modified calcium- and strontium phosphates

In the calcium phosphate system there is a limited range for substituting calcium by strontium in apatite due to the different ion radii of the

elements. Tadier et al. investigated the incorporation of strontium in apatite setting mineral bone cements via exchange of up to 20 wt% vaterite ($CaCO_3$) by $SrCO_3$ leading to a maximum of 8 wt% Sr in the cement as well as incorporating $SrCl_2 \cdot 6H_2O$ to its maximum solubility in the liquid cement component leading to 6 wt% of strontium in the final cement.[35] They showed that only the $SrCl_2$ in liquid modification did not cause a separate mineral phase in crystal structure analysis. Schumacher et al. showed the same with another apatite setting bone cement substituting the whole amount of $CaCO_3$ by $SrCO_3$ (8.5 wt% of the cement powder), which lead to a high degree of strontium doping, poor apatite crystallinity and still remaining $SrCO_3$ after setting.[36] In calcium phosphate cements which are hardening to single-phase brushite, Alkhraisat et al. observed the transition to strontium-substituted monetite with increasing strontium amounts.[37] Here the substitution of up to a quarter of the stoichiometric calcium by strontium in the finally formed monetite was achieved in case of classical re-precipitation. In the monetite, strontium ions are embedded in the crystal lattice. In the present case, the XRD results prove only slight changes of crystallography of brushite for C 10:0, C + S 9:1, and C + S 5:5. The same is true for increased amounts of Ca in $SrHPO_4$ in case of C + S 3:7, C + S 1:9, and S 10:0. It is important to notice, that not only ion substitution, but also formation of x-ray amorphous nano-crystals or amorphous mineral phases may cause the high foreign ion contents in the specimens as identified in ICP-OES measurements.

Mineral formation using either a pure calcium chloride mineralization solution or a mineralization solution containing 50% calcium chloride and 50% strontium chloride led to the formation of brushite with possibly minor strontium substitution according to XRD, FT-IR and previously published EDX results.[13,38] In addition, there are indications for an amorphous strontium phosphate phase in C + S 5:5. The assignment of $SrHPO_4$ for the S 0:10 mineral was made according to the publications of Wang et al., Zhuang et al. and Roming et al..[30-32]

The mineral formation was analyzed by SEM and ICP-OES to determine the morphological changes and real Ca/Sr ratios (by weight and molar fractions) in the specimens. The platelet-shaped particles of the calcium-rich minerals (C 10:0, C + S 9:1, C + S 5:5), which are very similar from a morphological point of view, show a disturbed crystal structure owing to strontium substitution. This is mainly indicated by the reduced edge sharpness at C + S 9:1 and C + S 5:5. In comparison, there is the group of strontium-based minerals C + S 3:7, C + S 1:9 and S 0:10, in which up to 10 wt% strontium (molar fraction of 21%) could be substituted by calcium (C + S 3:7). This goes also along with a reduced particle size and a disturbed structure of the rosette-shaped round particles of S 0:10.

The mineral precipitation during synthesis caused identical phosphorus content for all mineral variants. This might be caused by the fact that the initial molar amount of phosphorous (0.09 mol) in the gelatin phosphate solution is less than half the molar amount of calcium or strontium (0.25 mol).

Considering the twice as high atomic mass of strontium in comparison to calcium, both extremes C 10:0 and S 0:10 have a similar molar ratio between Ca and P as well as Sr and P of ~1. This indicates synthesis of calcium and strontium hydrogen phosphate, respectively, which was proven by XRD. The molar ratio between Ca + Sr and P of ~1 is also maintained in the mixed C + S x:y variants. However, the dry masses of specimen (Figure 3), the graph of the Ca/Sr ratio in the mineralization solutions and the measured calcium content in the specimen (Figure 4b), the FT-IR (Figure 5), and XRD (Figure 6) results give evidence for a division into two material groups. Thus, there are the variants C 10:0, C + S 9:1, C + S 5:5 assigned to the high-calcium minerals (brushite based), which allow a high but slightly decreasing degree of strontium substitution and amount up to a real molar Ca/Sr ratio of 79.8%/20.2%. The second groups are the ($SrHPO_4$ based) minerals with a high strontium content S 0:10, C + S 1:9 and C + S 3:7, which allow a certain degree of strontium substitution by calcium. There is a linear trend with a maximum Ca/Sr ratio of 20.9%/79.1% (C + S 3:7 in Figure 4b).

Both strontium substitution of C 10:0 and calcium substitution of S 0:10 led to a significant influence on biomaterial degradation and strength.

4.2 | Material degradation and mechanical strength

The degradation characteristics of bone substitute materials in selected electrolyte solutions and the associated mechanical strength provide an initial indicator of the in vivo behavior of the material. The results presented above thus allow a selection for cell culture investigations and clearly show that there is a functional relationship between the material composition, structure, morphology, and microstructure, strongly influenced by the Ca/Sr ratio. There is no doubt that the degradation behavior in vivo differs significantly from that in vitro, mainly due to the large number of different cells present in the bone multicellular unit during bone remodeling. Nevertheless, in vitro degradation studies provide important information on possible changes to the material as a result of physicochemical dissolution and re-precipitation of once dissolved substances.

When interpreting the degradation processes described here, however, the mineral precipitation process from the electrolyte solutions can be neglected, since the total mass of calcium and phosphate, which can potentially precipitate out of the medium in form of hydroxyapatite, is ~1.4 mg. This amount was calculated assuming that the whole amount of calcium or phosphorous would precipitate as hydroxyapatite from the 8 ml medium. This is clearly smaller than the actual measured mass changes of the test specimens of 12 mg on average.

The extent of mineral precipitation typically characterizes the so-called bioactive state of the specimens,[39,40] but in the present case the effect of mineral dissolution and re-precipitation is significantly greater on mechanical stability and ion concentrations than on the change in mass. The released calcium and phosphate ions during material degradation partly contribute to the mechanical stabilization of the specimens, as the measurement of the indirect tensile strength shows. This effect is greatest with the smaller particles of C + S 5:5. In the previously mentioned calcium phosphate cements according to Driessens,[41] the described re-precipitation is used to harden the cements, whereby the remaining phases, in particular hydroxyapatite, act as a heterogeneous nucleating agent. In addition, the strontium substitution of calcium phosphate cements has shown a similar increase in strength.[36] To ensure that this process does not take place after days—as it is the case for C 10:0, C + S 9:1, and C + S 5:5—but in minutes, an alkaline phase is added to the acid calcium phosphate phase of calcium phosphate cements, whereby the ratio of the components is determined via the Ca/P ratio. According to Fernández et al.[42] this is responsible for the setting of the cement to brushite or calcium-deficient HAp. The occurring transformation and mineral precipitation influences the pH value, which is why the pH value reduction for C 10:0, C + S 9:1, and C + S 5:5 is in direct correlation with the increase in mechanical strength and phosphate release. In detail, the solution contains an equilibrium of $H_2PO_4^-$ and HPO_4^{2-} ions. According to Recillas et al. precipitation of monetite, brushite, or (calcium-deficient) HAp is generally possible at the given pH according to the calcium and phosphate ion concentrations.[43] Nevertheless, at the given pH of the medium at the begin of about 8.1 and even during degradation (pH > 6.8) hydroxyapatite is most likely to precipitate. During the precipitation from the supersaturated medium on the specimen, HPO_4^{2-} or PO_4^{3-} ions are removed from the medium, while reacting with Ca^{2+}. The dissolution of the material and precipitation of calcium phosphates goes along with the increase of hydronium

ions, which lowers the pH value. The increased ratio of Ca/P in $Ca_5(PO_4)_3(OH)$ (HAP, 1.67:1) compared to the present $CaHPO_4 \cdot 2H_2O$ (calcium hydrogen phosphate, 1:1) leads to a decrease of the calcium concentration while the phosphate concentration increases at the same time owing to parallel specimen dissolution and mineral precipitation.

However, these effects are comparatively small for specimens with a high strontium content. Since no strontium is contained in the initial medium, supersaturation with regard to strontium phosphate precipitation does not occur during static incubation. Therefore, no hardening by precipitation of the specimens with a higher strontium content can be detected and the strength decreases due to degradation. Compared with brushite and monetite, $SrHPO_4$ shows a lower solubility in aqueous solutions, which has been proven by Aia et al.[44] in a temperature range of 25–90°C. The lower solubility leads to a smaller decrease in mass of S 0:10, C + S 1:9 and C + S 3:7 compared to the high-calcium containing minerals. In addition, in this case the calcium substitution leads to an increased solubility and degradation due to the disturbed crystal structure. Furthermore, strontium is an inhibitor of apatite formation, which was proven for gelatin-containing calcium phosphate cements hardening to calcium deficient hydroxyapatite.[45] This may be the reason for smaller changes of mechanical strength occurring in the strontium-rich samples.

5 | CONCLUSIONS

In summary, the degradation studies show that the pure calcium phosphates (C 10:0) as well as the high-calcium containing phosphates (C + S), both gelatin modified, cannot provide the desired amount of calcium ions for fracture healing as a result of their degradation. An increase of calcium concentration leads to an exceeding the solubility limits in the ambient solution and thus to the precipitation of already dissolved calcium phosphates on the material acting as nucleation germ.

Minerals containing ions other than calcium, such as strontium, can increase the activity of osteoblasts by releasing them. Of particular interest in this context are the highly substituted mineral variants, that is, C + S 5:5 with a real molar Ca/Sr ratio of 20%/80% (63%/37% by element mass) and C + S 3:7 with a molar Ca/Sr ratio of 21%/79% (10%/90% by element mass). These materials are characterized by a maximum initial cation release during incubation, a high initial strength and they allow a targeted adjustment of phosphate release and material degradation by tuning particle size and morphology. At the same time, material-based manipulation of the cation concentration in the implant vicinity can be used perspectively to influence cellular reactions of osteoblasts and osteoclasts in the bone-multicellular unit during the remodeling process.

ORCID
Benjamin Kruppke 🆔 https://orcid.org/0000-0002-0659-0238

REFERENCES

1. Du Y, Guo JL, Wang J, Mikos AG, Zhang S. Hierarchically designed bone scaffolds: From internal cues to external stimuli. *Biomaterials*. 2019;*218*:119334. https://doi.org/10.1016/j.biomaterials.2019.119334.

2. Van Bommel KJC, Friggeri A, Shinkai S. Organic templates for the generation of inorganic materials. *Angew Chem Int Ed*. 2003;*42*:980-999. https://doi.org/10.1002/anie.200390284.

3. Heinemann C, Heinemann S, Kruppke B, et al. Electric field-assisted formation of organically modified hydroxyapatite (ormoHAP) spheres in carboxymethylated gelatin gels. *Acta Biomater*. 2016;*44*:135-143. https://doi.org/10.1016/j.actbio.2016.08.024.

4. Nudelman F, Sommerdijk NAJM. Biomineralization as an inspiration for materials chemistry. *Angew Chem Int Ed*. 2012;*51*:6582-6596. https://doi.org/10.1002/anie.201106715.

5. Kollmann T, Simon P, Carrillo-Cabrera W, et al. Calcium phosphate - gelatin Nanocomposites: bulk preparation (shape- and phase-control), characterization, and application as dentine repair material. *Chem Mater*. 2010;*22*:5137-5153. https://doi.org/10.1021/cm101755j.

6. Tamimi F, Sheikh Z, Barralet J. Dicalcium phosphate cements: brushite and monetite. *Acta Biomater*. 2012;*8*:474-487. https://doi.org/10.1016/j.actbio.2011.08.005.

7. Habraken W, Habibovic P, Epple M, Bohner M. Calcium phosphates in biomedical applications: materials for the future? *Mater Today*. 2016;*19*:69-87. https://doi.org/10.1016/j.mattod.2015.10.008.

8. Montazerolghaem M, Karlsson Ott M, Engqvist H, Melhus H, Rasmusson AJ. Resorption of monetite calcium phosphate cement by mouse bone marrow derived osteoclasts. *Mater Sci Eng C*. 2015;*52*:212-218. https://doi.org/10.1016/j.msec.2015.03.038.

9. Gisep A, Wieling R, Bohner M, Matter S, Schneider E, Rahn B. Resorption patterns of calcium-phosphate cements in bone. *J Biomed Mater Res - Part A*. 2003;*66*:532-540. https://doi.org/10.1002/jbm.a.10593.

10. Apelt D, Theiss F, El-Warrak AO, et al. In vivo behavior of three different injectable hydraulic calcium phosphate cements. *Biomaterials*. 2004;*25*:1439-1451. https://doi.org/10.1016/j.biomaterials.2003.08.073.

11. B. Ben-Nissan, *Advances in Calcium Phosphate Biomaterials*, SpringerBerlin Heidelberg, Berlin, Heidelberg, 2014. https://doi.org/10.1007/978-3-642-53980-0.

12. Gbureck U, Hölzel T, Klammert U, Würzler K, Müller FA, Barralet JE. Resorbable dicalcium phosphate bone substitutes prepared by 3D powder printing. *Adv Funct Mater*. 2007;*17*:3940-3945. https://doi.org/10.1002/adfm.200700019.

13. Kruppke B, Farack J, Wagner A-S, et al. Gelatine modified monetite as a bone substitute material: An in vitro assessment of bone biocompatibility. *Acta Biomater*. 2016;*32*:275-285. https://doi.org/10.1016/j.actbio.2015.12.035.

14. Hoppe A, Güldal NS, Boccaccini AR. A review of the biological response to ionic dissolution products from bioactive glasses and glass-ceramics. *Biomaterials*. 2011;*32*:2757-2774. https://doi.org/10.1016/j.biomaterials.2011.01.004.

15. Schumacher M, Lode A, Helth A, Gelinsky M. A novel strontium(II)-modified calcium phosphate bone cement stimulates human-bone-marrow-derived mesenchymal stem cell proliferation and osteogenic differentiation in vitro. *Acta Biomater*. 2013;*9*:9547-9557. https://doi.org/10.1016/j.actbio.2013.07.027.

16. Luo X, Barbieri D, Duan R, Yuan H, Bruijn JD. Strontium-containing apatite/polylactide composites enhance bone formation in osteopenic rabbits. *Acta Biomater*. 2015;*26*:331-337. https://doi.org/10.1016/j.actbio.2015.07.044.

17. Marie PJ. Strontium as therapy for osteoporosis. *Curr Opin Pharmacol*. 2005;*5*:633-636. https://doi.org/10.1016/j.coph.2005.05.005.

18. Pors Nielsen S. The biological role of strontium. *Bone*. 2004;*35*:583-588. https://doi.org/10.1016/j.bone.2004.04.026.

19. Ray S, Thormann U, Sommer U, et al. Effects of macroporous, strontium loaded xerogel-scaffolds on new bone formation in critical-size metaphyseal fracture defects in ovariectomized rats. *Injury*. 2016;*47*(Suppl 1):52-61. https://doi.org/10.1016/S0020-1383(16)30013-4.

20. Skoryna SC. Effects of oral supplementation with stable strontium. *Can Med Assoc J*. 1981;*125*:703-712.

21. Reginster JY, Seeman E, De Vernejoul MC, et al. Strontium ranelate reduces the risk of nonvertebral fractures in postmenopausal women with osteoporosis: Treatment of peripheral osteoporosis (TROPOS) study. *J Clin Endocrinol Metab*. 2005;*90*:2816-2822. https://doi.org/10.1210/jc.2004-1774.

22. Neves N, Linhares D, Costa G, Ribeiro CC, Barbosa MA. *In vivo* and clinical application of strontium-enriched biomaterials for bone regeneration. *Bone Jt Res*. 2017;*6*:366-375. https://doi.org/10.1302/2046-3758.66.BJR-2016-0311.R1.

23. Verberckmoes SC, De Broe ME, D'Haese PC. Dose-dependent effects of strontium on osteoblast function and mineralization. *Kidney Int*. 2003;*64*:534-543. https://doi.org/10.1046/j.1523-1755.2003.00123.x.

24. Bonnelye E, Chabadel A, Saltel F, Jurdic P. Dual effect of strontium ranelate: Stimulation of osteoblast differentiation and inhibition of osteoclast formation and resorption in vitro. *Bone*. 2008;*42*:129-138. https://doi.org/10.1016/j.bone.2007.08.043.

25. Bizelli-Silveira C, Pullisaar H, Abildtrup LA, et al. Strontium enhances proliferation and osteogenic behavior of periodontal ligament cells in vitro. *J Periodontal Res*. 2018;*53*:1020-1028. https://doi.org/10.1111/jre.12601.

26. Bizelli-Silveira C, Abildtrup LA, Spin-Neto R, Foss M, Søballe K, Kraft DCE. Strontium enhances proliferation and osteogenic behavior of bone marrow stromal cells of mesenchymal and ectomesenchymal origins in vitro. *Clin Exp Dent Res*. 2019;*5*:1-10. https://doi.org/10.1002/cre2.221.

27. Canalis E, Hott M, Deloffre P, Tsouderos Y, Marie PJ. The divalent strontium salt S12911 enhances bone cell replication and bone formation in vitro. *Bone*. 1996;*18*:517-523. https://doi.org/10.1016/8756-3282(96)00080-4.

28. Kruppke B, Wagner AS, Heinemann C, et al. Strontium ions promote in vitro human bone marrow stromal cell proliferation and differentiation in calcium-lacking media. *Develop Growth Differ*. 2018;*61*:166-175. https://doi.org/10.1111/dgd.12588.

29. Catti M, Ferraris G, Filhol A. Hydrogen bonding in the crystalline state. CaHPO4 (monetite), P1 or P1? A novel neutron diffraction study. *Acta Crystallogr Sect B Struct Crystallogr Cryst Chem*. 1977;*33*:1223-1229. https://doi.org/10.1107/S0567740877005706.

30. WANG M, TIAN B, YUE D, et al. Crystal structure, morphology and luminescent properties of rare earthion-doped SrHPO4 nanomaterials. *J Rare Earths*. 2015;*33*:355-360. https://doi.org/10.1016/S1002-0721(14)60426-9.

31. Zhuang FQ, Tan RQ, Shen WF, Zhang XP, Xu W, Song WJ. Synthesis of β-type strontium hydrogen phosphate nanosheets and its immobilization of Pb2+ in acidic aqueous solution. *Acta Metall Sin*. 2015;*28*:438-443. https://doi.org/10.1007/s40195-015-0214-z.

32. Roming M, Feldmann C. Selective synthesis of α- and β-SrHPO4 nanoparticles. *J Mater Sci*. 2008;*43*:5504-5507. https://doi.org/10.1007/s10853-008-2830-8.

33. Brock CP, Hahn T, Wondratschek H, et al. *International Tables for Crystallography Volume A: Space-Group Symmetry*. Dordrecht, The Netherlands: International Union of Crystallography; 2019.

34. A.A. Coelho, TOPAS-Academic, (2016). http://www.topas-academic.net/.

35. Tadier S, Bareille R, Siadous R, et al. Strontium-loaded mineral bone cements as sustained release systems: compositions, release properties, and effects on human osteoprogenitor cells. *J Biomed Mater Res - Part B Appl Biomater*. 2012;*100*:378-390. https://doi.org/10.1002/jbm.b.31959.

36. Schumacher M, Henß A, Rohnke M, Gelinsky M. A novel and easy-to-prepare strontium(II) modified calcium phosphate bone cement with enhanced mechanical properties. *Acta Biomater*. 2013;*9*:7536-7544. https://doi.org/10.1016/j.actbio.2013.03.014.

37. Hamdan Alkhraisat M, Moseke C, Blanco L, Barralet JE, Lopez-Carbacos E, Gbureck U. Strontium modified biocements with zero order release kinetics. *Biomaterials*. 2008;*29*:4691-4697. https://doi.org/10.1016/j.biomaterials.2008.08.026.

38. Kruppke B, Wagner A-S, Rohnke M, et al. Biomaterial based treatment of osteoclastic/osteoblastic cell imbalance – gelatin-modified calcium/strontium phosphates. *Mater Sci Eng C*. 2019;*104*:109933. https://doi.org/10.1016/j.msec.2019.109933.

39. Bohner M, Lemaitre J. Can bioactivity be tested in vitro with SBF solution? *Biomaterials*. 2009;*30*:2175-2179. https://doi.org/10.1016/j.biomaterials.2009.01.008.

40. Kokubo T, Takadama H. How useful is SBF in predicting in vivo bone bioactivity? *Biomaterials*. 2006;*27*:2907-2915. https://doi.org/10.1016/j.biomaterials.2006.01.017.

41. Driessens FCM, Planell JA, Boltong MG, Khairoun I, Ginebra MP. Osteotransductive bone cements. *Proc Inst Mech Eng Part H J Eng Med*. 1998;*212*:427-435. https://doi.org/10.1243/0954411981534196.

42. Fernández E, Gil FJ, Best S, Ginebra MP, Driessens FC, Planell JA. The cement setting reaction in the CaHPO4-alpha-Ca3(PO4)2 system: an X-ray diffraction study. *J Biomed Mater Res*. 1998;*42*:403-406.

43. Recillas S, Rodríguez-Lugo V, Montero ML, Viquez-Cano S, Hernandez L, Castaño VM. Studies on the precipitation behavior of calcium phosphate solutions. *J Ceram Process Res*. 2012;*13*:5-10.

44. Aia MA, Mathers JE, Mooney RW. Thermodynamic solubility products of α- and β-SrHPO4 from 25 °C to 90 °C. *J Chem Eng Data*. 1964;*9*:335-338. https://doi.org/10.1021/je60022a006.

45. Panzavolta S, Torricelli P, Sturba L, Bracci B, Giardino R, Bigi A. Setting properties and in vitro bioactivity of strontium-enriched gelatin-calcium phosphate bone cements. *J Biomed Mater Res - Part A*. 2008;*84*:965-972. https://doi.org/10.1002/jbm.a.31412.

SUPPORTING INFORMATION

Additional supporting information may be found online in the Supporting Information section at the end of this article.